

# Tetracyanomethane under Pressure: Extended CN Polymers from Precursors with Built-in $sp^3$ Centers

Derek W. Keefer,<sup>\*,†</sup> Huiyang Gou,<sup>⊥,%</sup> Qianqian Wang,<sup>⊥</sup> Andrew Purdy,<sup>#</sup> Albert Epshteyn,<sup>#</sup> Stephen J. Juhl,<sup>†</sup> George D. Cody,<sup>⊥</sup> John Badding,<sup>†,‡,§,||</sup> and Timothy A. Strobel<sup>\*,⊥</sup>

HPSTAR  
548-2018

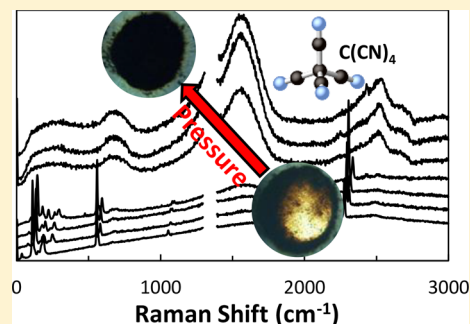
<sup>†</sup>Department of Chemistry, <sup>‡</sup>Department of Physics, <sup>§</sup>Department of Materials Science and Engineering, and <sup>||</sup>Materials Research Institute, The Pennsylvania State University, University Park, Pennsylvania 16802, United States

<sup>⊥</sup>Geophysical Laboratory, Carnegie Institution of Washington, 5251 Broad Branch Road NW, Washington, D.C. 20015, United States

<sup>#</sup>Chemistry Division, Naval Research Laboratory, 4555 Overlook Ave., SW, Washington, D.C. 20375, United States

<sup>%</sup>Center for High Pressure Science and Technology Advanced Research, Beijing 100094, China

**ABSTRACT:** Tetracyanomethane,  $C(CN)_4$ , is a tetrahedral molecule containing a central  $sp^3$  carbon that is coordinated by reactive nitrile groups that could potentially transform to an extended CN network with a significant fraction of  $sp^3$  carbon. High-purity  $C(CN)_4$  was synthesized, and its physicochemical behavior was studied using *in situ* synchrotron angle-dispersive powder X-ray diffraction (PXRD) and Raman and infrared (IR) spectroscopies in a diamond anvil cell (DAC) up to 21 GPa. The pressure dependence of the fundamental vibrational modes associated with the molecular solid was determined, and some low-frequency Raman modes are reported for the first time. Crystalline molecular  $C(CN)_4$  starts to polymerize above  $\sim 7$  GPa and transforms into an interconnected disordered network, which is recoverable to ambient conditions. The results demonstrate feasibility for the pressure-induced polymerization of molecules with premeditated functionality.



## INTRODUCTION

The carbon–nitrogen (CN) system has many similarities with pure carbon. For example, both systems possess (or are predicted to possess) two-dimensional, soft allotropes (graphite and graphitic carbon nitride) as well as three-dimensional, superhard allotropes (diamond and cubic carbon nitride).<sup>1,2</sup> The structural dimensionality and resulting physical properties are directly determined by the degree to which bonding hybridization takes on  $sp^2$  and/or  $sp^3$  forms. For CN materials, several techniques have been demonstrated for the synthesis of  $sp^2$  materials; however, significant challenges remain to produce three-dimensional extended materials with  $sp^3$  hybridization.<sup>3–9</sup>

There are several approaches to synthesize carbon nitride extended solids, such as soft chemical methods, magnetron sputtering, high-pressure techniques, etc. Generally,  $sp^2$  hybridized graphitic  $C_3N_4$  ( $g-C_3N_4$ ), which is considered to be a promising low-cost, metal-free, visible-light-active photocatalyst, can be synthesized through chemical methods, such as thermal condensation of nitrogen-rich and oxygen-free compounds containing C–N core structures (e.g., cyanamide, dicyandiamide, melamine, thiourea, or urea).<sup>10,11</sup> Amorphous or fullerene-like  $CN_x$  thin films are typically fabricated by magnetron sputtering methods with interesting mechanical properties, such as high hardness and elastic recovery.<sup>12–18</sup> Incorporation of nitrogen is considered to be helpful for the formation of fullerene-like microstructure and the cross-linking between graphitic layers by  $sp^3$  coordinated carbon in the

carbon nitride films that contribute to the high hardness and elastic recovery. High pressure is also an alternative method to produce carbon nitride solids, such as the polymerization of different high-energy, unsaturated molecules under pressure.<sup>19–24</sup> In most high-pressure studies, amorphous  $sp^2$  bonded carbon nitride is obtained with some  $sp^3$  bonded carbon. The recent high-pressure synthesis of crystalline orthorhombic CN and tetragonal  $C_3N_4$  phases with  $sp^3$  hybridization shows promise for the formation of new superhard materials and bonding motifs that span three dimensions.<sup>25,26</sup> An alternative approach to achieving CN solids with an increased fraction on  $sp^3$  bonds could be to start with inherently three-dimensional precursor molecules that could be designed to react to form extended networks. In this case, the reaction process would occur in the bulk, and samples might be scalable in quantities beyond that which is possible for thin films.

Tetracyanomethane was originally synthesized and characterized by Mayer ca. 1968.<sup>27</sup> Since cyanogen chloride is not commercially available, we used cyanogen bromide instead and obtained  $C(CN)_4$  in about 50% yield. The molecule has tetrahedral symmetry and contains a central  $sp^3$  carbon that is coordinated by reactive nitrile groups that are capable of

Received: October 30, 2017

Revised: January 11, 2018

Published: February 12, 2018

transforming to a hydrogen-free, three-dimensional extended CN network with a significant fraction of  $sp^3$  carbon. It is well established that cyanide groups can undergo thermally and/or pressure-induced polymerization reactions; however, starting precursor molecules generally lack 3D/intrinsic  $sp^3$  character, and the resulting extended CN phases are typically  $sp^2$ , even under elevated pressure conditions.<sup>19,21,22,24,28–34</sup>

In this study, we examine the behavior of  $C(CN)_4$  under compression using Raman, IR, and PXRD up to 20 GPa and test the hypothesis of whether extended 3D networks can be produced by reaction of a 3D precursor. Raman and IR spectroscopy provide *in situ* information on how the bonding develops, while synchrotron PXRD was used to monitor how the structure progresses. *Ex situ* electron microscopy measurements were performed to characterize the recovered product.

## EXPERIMENTAL METHODS

A solution of  $AgNO_3$  (7.19 g, 42.3 mmol) in 70 g of  $H_2O$  was added to a solution of  $KC(CN)_3$  (Strem, 5.40 g, 41.8 mmol) in 65 g of  $H_2O$  with vigorous stirring and was allowed to stir for 12 h. The mixture was filtered, and the white solid washed with water and alcohol and pumped dry while heating with warm water for several hours.  $AgC(CN)_3$  (7.90 g, 95%) was isolated.

Cyanogen bromide (2.50 g, 23.6 mmol) was transferred under vacuum onto  $AgC(CN)_3$  (3.42 g, 17.3 mmol) in a large Pyrex tube. The tube was sealed under vacuum and immersed in a 100 °C oil bath for 11 days. The tube was opened in the drybox, and the contents were sublimed under dynamic vacuum using a 100 °C oil bath and an ice-cooled coldfinger. A total of 1.081 g of  $C(CN)_4$  was isolated (54%). NMR:  $(CD_3CN)$   $^{13}C$   $\delta$  103.2 ( $C\equiv N$ ), 22.7 (C). Tetracyanomethane is very water sensitive and was handled only in the drybox.

**Sample Preparation.** Samples of tetracyanomethane were ground to a fine powder ( $<1 \mu m$ ) using an agate mortar within an argon glovebox ( $O_2 < 0.5$  ppm,  $H_2O < 0.5$  ppm). This powder, with the addition of a ruby sphere, was placed into a DAC gasket chamber with culet sizes ranging between 300 and 500  $\mu m$ . A rhenium gasket was prepared by preindentation to a thickness between 50 and 70  $\mu m$ . An  $\sim 150$ – $190 \mu m$  hole was drilled into the center of the indentation, which served as the chamber for the sample. By measuring the fluorescence of the ruby sphere, the pressure inside the sample chamber could be determined.<sup>35</sup> In most runs, a pressure transmitting medium was not used, but dry potassium bromide was used to dilute samples for some of the IR runs to avoid absorbance saturation. To prevent reaction/contamination with moisture in air, all samples were sealed inside the glovebox at a minimum pressure of 0.1 GPa.

**Raman.** Raman spectra were collected in the backscattered geometry with excitation from a 532 nm diode laser. The light was focused through a 20 $\times$  long working distance objective (NA = 0.40) and collected through a 50  $\mu m$  confocal pinhole and two narrow-band notch filters (Ondax). A Princeton Instrument spectrograph SP2750 (Trenton, NJ) with 1800 or 300 grooves/mm grating and a liquid-nitrogen-cooled CCD was used to collect data with a spectral resolution of  $<2 \text{ cm}^{-1}$ . Neon emission lines were used to calibrate the spectrometer to an accuracy of  $<1 \text{ cm}^{-1}$ . To avoid damaging the sample, laser power was kept below 5 mW, and exposure times were varied up to 300 s. At higher laser power, it was observed that the laser could help promote reaction progress at high pressure.

**Infrared.** Mid-IR absorption from 600 to 4000  $\text{cm}^{-1}$  was collected on a Varian 670-IR spectrometer. A Globar source

was used to generate IR light, which was then focused through a pair of reflecting objectives. The signal was detected using a liquid-nitrogen-cooled HgCdTe detector. After the data were collected, the same DAC was decompressed, the diamonds were cleaned, and reference spectra were collected.

**X-ray Diffraction.** Powder X-ray diffraction (PXRD) data were obtained at the High-Pressure Collaborative Access Team (HPCAT), beamline 16-IDB, of the Advanced Photon Source (APS), Argonne National Laboratory. Data were collected with a monochromatic beam with a wavelength of 0.4066 Å and focused to  $\sim 5 \times 7 \mu m^2$  spot. Diffraction data were recorded using a MARCCD, and the images were processed using the FIT2D(v12.077) data analysis program.<sup>36</sup> Lattice parameters were obtained through full-profile fitting using the Le Bail method, as implemented in GSAS with EXPGUI.<sup>37,38</sup>

**Scanning and Transmission Electron Microscopy.** The recovered samples within the Re gaskets were mounted on an Al stub for chemical composition mapping and microstructural analysis using a field emission scanning electron microscope (FE-SEM; JEOL JSM 6500F) operating at 15 kV and 1.5 nA. Compositional analyses were determined by energy-dispersive X-ray spectroscopy (EDS) using graphite and BN standards.

Transmission electron microscope (TEM) bright-field imaging was performed using a JEOL 2010 microscope with a  $LaB_6$  electron source operating under an accelerating voltage of 200 kV. Samples were carefully removed from the Re gasket using a steel needle, mechanically crushed on a piece of Teflon, and then dispersed onto a silicon monoxide grid with ethanol.

## RESULTS AND DISCUSSION

Tetracyanomethane is a molecular solid at ambient conditions and was previously reported to crystallize in a trigonal lattice with space group  $R3c$  (No. 161) and six formula units per unit cell.<sup>39</sup> The crystal structure may be viewed as a distortion from cubic symmetry due to the weak intermolecular interactions that benefit from the denser trigonal structure.<sup>39</sup> Tetracyanomethane molecules maintain tetrahedral symmetry in the solid phase. The molecules are stacked with the nitrile groups pointing toward the central carbon of an adjacent molecule along the  $c$ -axis. Figure 1 shows the crystal structure of  $C(CN)_4$  with nearest-neighbor interaction distances. There are several short intermolecular distances near 3 Å (3.00, 3.05, 3.10, and

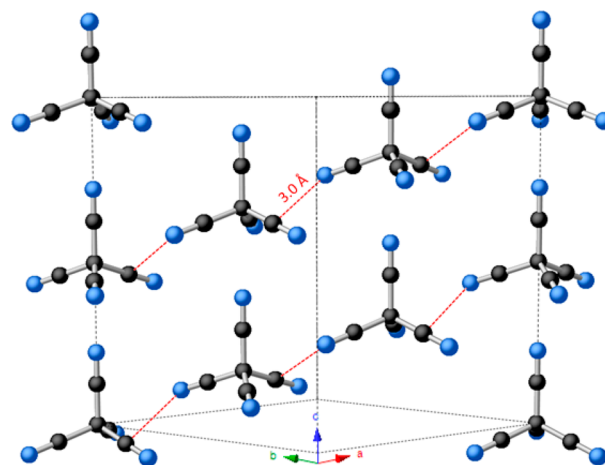


**Figure 1.** Crystal structure of  $C(CN)_4$  with nearest-neighbor interactions shown as red dashed lines. Every C/N nitrile atom has three interactions with adjacent molecules near 3.0 Å.

3.19 Å) between the nitrogen atoms and nitrile carbon atoms of neighboring molecules.<sup>24</sup>

PXRD patterns obtained from the starting material at 0.1 GPa were readily refined using the trigonal structural model, and the resulting lattice parameters of  $a = 8.951(2)$  Å and  $c = 11.54(4)$  Å are in good agreement with the previously reported results at ambient conditions.<sup>39</sup> Figure 2 shows the trends in

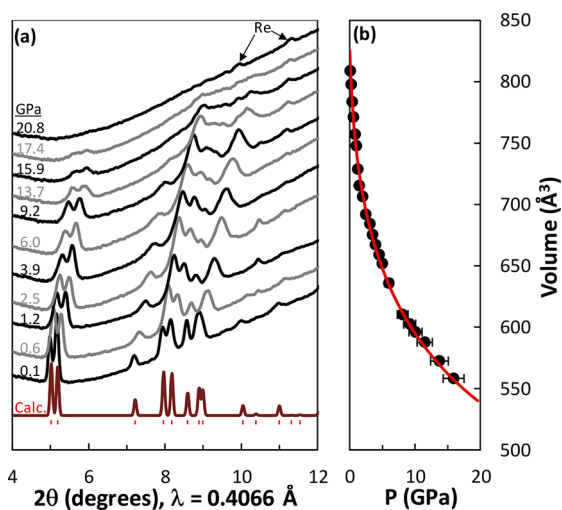


**Figure 2.** (a) PXRD of  $C(CN)_4$  as a function of pressure up to 20 GPa. Small peaks from the Re gasket are visible in some high-pressure patterns. The calculated starting pattern is shown below. (b) Unit cell volume for the  $R3c$  structure with pressure. Solid line is the fitted EoS.

the PXRD patterns as the material was compressed up to 20 GPa. With increasing pressure, the Bragg peaks broaden due to nonhydrostatic compression and anisotropic microstrain (no pressure medium was used), yet no structural phase transition was observed, and we were able to reliably refine the trigonal lattice parameters up to a pressure of 14.7 GPa. The lattice parameters  $a$  and  $c$  both decrease in a manner that is typical for a molecular solid. The pressure–volume relationship (Figure

2b) was fitted using the third-order Birch–Murnaghan equation of state (EoS)<sup>40</sup> with a bulk modulus of  $K_0 = 4.4(3)$  and derivative of  $K_0' = 18(1)$ . Above 14.7 GPa the diffraction intensity decreases drastically, and the material appears to be amorphous to X-rays above 20 GPa, although no clear diffuse scattering signal was detectable beyond the Compton scattering background produced by the diamond anvils.

The isolated tetracyanomethane molecule has 21 fundamental vibrational modes. As a crystalline solid in the  $R3c$  structure, the irreducible representation of all zone-center modes is given as  $M = 9A_1 + 9A_2 + 18E$ , of which 24 ( $A_1, E$ ) optic modes are both Raman- and IR-active. For comparison purposes, we report mode numbers following fundamental assignments for the isolated molecule, i.e.,  $2A_1(R) + 2E(R) + F_1(\text{silent}) + 4F_2(\text{IR,R})$ ; however, some of these fundamentals were observed to split in the solid due to crystal-field effects. Table 1 shows frequencies of observed Raman and IR modes compared with previous results from the literature.

At our starting pressure of  $\sim 0.1$  GPa, the observed Raman and IR modes are in general agreement with the previous studies.<sup>41,42</sup> From a molecular perspective, we follow the mode numbering scheme of Gardiner et al.<sup>42</sup> in which the  $\nu_5(F_1)$  C–C–C deformation is silent, whereas Hester et al.<sup>41</sup> assigned  $\nu_5$  to the  $C\equiv N$  asymmetric stretch ( $\nu_6$  here). We observed that the Raman-active C–C symmetric stretch ( $\nu_2$ ) split into three peaks at 561, 562, and 563  $\text{cm}^{-1}$ , whereas Hester et al.<sup>41</sup> only reported a very weak peak at 560  $\text{cm}^{-1}$ . Similarly, we resolved two peaks for C–C asymmetric stretching ( $\nu_7$ ) at 1059 and 1063  $\text{cm}^{-1}$  in the Raman and at 1058 and 1062  $\text{cm}^{-1}$  in the IR, whereas a single broad peak located at 1056  $\text{cm}^{-1}$  (IR + R) was reported previously.<sup>41</sup> We did not observe  $\nu_8$  and  $\nu_9$ , but Gardiner et al.<sup>42</sup> reported their positions from solution (acetonitrile) IR measurements at 540 and 478  $\text{cm}^{-1}$ , respectively. We observed four Raman lattice modes at 192, 176, 156, and 43  $\text{cm}^{-1}$ . Hester et al.<sup>41</sup> reported the same three higher-frequency lattice modes as well as an additional feeble mode at 75  $\text{cm}^{-1}$ . Some differences in frequency are naturally expected based upon differences in measurement pressure, i.e., 1 bar vs 1000 bar, but the crystal structure remains unchanged.

**Table 1. Experimental Raman and IR Modes Observed for Tetracyanomethane at  $\sim 0.1$  GPa**

vibrational mode	character	Raman (R), infrared (IR)	exptl observations ( $\text{cm}^{-1}$ ) (*solid, **solution, ***vapor)	
			this study	literature
$\nu_1 (A_1)$	$\nu_s (N\equiv C)$	R	2285	2288* <sup>41</sup>
$\nu_2 (A_1)$	$\nu_s (C-C)$	R	561, 562, 563	562* <sup>41</sup>
$\nu_3 (E)$	$\delta (C-C-N)$	R	572	573* <sup>41</sup>
$\nu_4 (E)$	$\delta (C-C-C)$	R	117	115* <sup>41</sup>
$\nu_5 (F_1)$	$\delta (C-C-C)$	N/A		136 <sup>42</sup>
$\nu_6 (F_2)$	$\nu_{as} (N\equiv C)$	R	2281	
		IR	2281	2276* <sup>41</sup> 2270*** <sup>41</sup>
$\nu_7 (F_2)$	$\nu_{as} (C-C)$	R	1059, 1063	1056* <sup>41</sup> 1061*** <sup>41</sup>
		IR	1058, 1062	1056* <sup>41</sup>
$\nu_8 (F_2)$	$\delta (C-C-N)$	R		
		IR		540** <sup>42</sup>
$\nu_9 (F_2)$	$\delta (C-C-N)$	R		
		IR		478** <sup>42</sup>
$\nu_L$	lattice	R	192	190* <sup>41</sup>
$\nu_L$	lattice	R	176	178* <sup>41</sup>
$\nu_L$	lattice	R	156	154* <sup>41</sup>
$\nu_L$	lattice	R	43	

<sup>a</sup>Calculated from normal coordinate analysis.<sup>26</sup>

The pressure dependence of Raman and IR modes is plotted in Figure 3. All modes show an overall trend of increasing

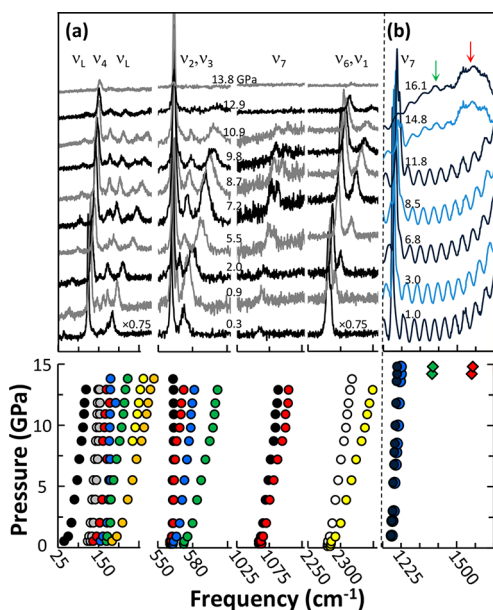


Figure 3. (a) Raman spectra of  $C(CN)_4$  with pressure. The pressure dependence of individual peaks is shown on the same scale below the spectra. (b) IR absorbance spectra of the  $\nu_7$  modes plotted with pressure. Oscillations are interference fringes between the two parallel diamond surfaces. Increasing absorbance above  $\sim 1500\text{ cm}^{-1}$  is from the diamond anvils. New broad features marked by arrows at  $\sim 1335$  and  $\sim 1600\text{ cm}^{-1}$  are clearly observed above 14 GPa. The pressure dependence of the peaks is shown in the panel below the spectra.

frequency with pressure. No abrupt discontinuities in frequency were observed with increasing pressure, although frequencies of individual modes do exhibit different pressure dependencies and thus different mode Grüneisen parameters. These observations indicate that  $C(CN)_4$  remains in the starting  $R3m$  structure and are in agreement with our PXRD results. Above  $\sim 12$  GPa the observed intensities of the fundamental Raman and IR modes decrease significantly, and above 14 GPa none of the original peaks are detectable. New broad IR features at  $\sim 1335$  and  $\sim 1600\text{ cm}^{-1}$  appear above 14 GPa.

In addition to the loss of Raman scattering and IR absorbance of fundamental modes above 12 GPa, new vibrational modes were observed above this pressure as well as dramatic color changes of the sample (Figure 4a). No color change was observed in the material between 0 and 11 GPa, but beyond this pressure the material begins to darken, eventually transforming to a completely opaque material above  $\sim 15$  GPa. The loss of fundamental vibrational modes combined with drastic color changes and X-ray amorphization point to a polymerization reaction and loss of molecular character. This chemical transformation was observed directly using *in situ* Raman and IR spectroscopy. When the broad-range Raman spectrum is plotted, new broad peaks are observed near  $\sim 670$  and  $1400\text{ cm}^{-1}$  that grow in intensity above  $\sim 7$  GPa while all other modes decrease in intensity (Figure 4b). Beyond 14 GPa, only these broad features are observed in the Raman as well as modes at  $\sim 1335$  and  $\sim 1600\text{ cm}^{-1}$  in the IR. The Raman feature near  $1400\text{ cm}^{-1}$  can be deconvoluted into D and G peaks, which are normally observed in amorphous carbon materials and indicate the reaction of the nitrile groups and the formation

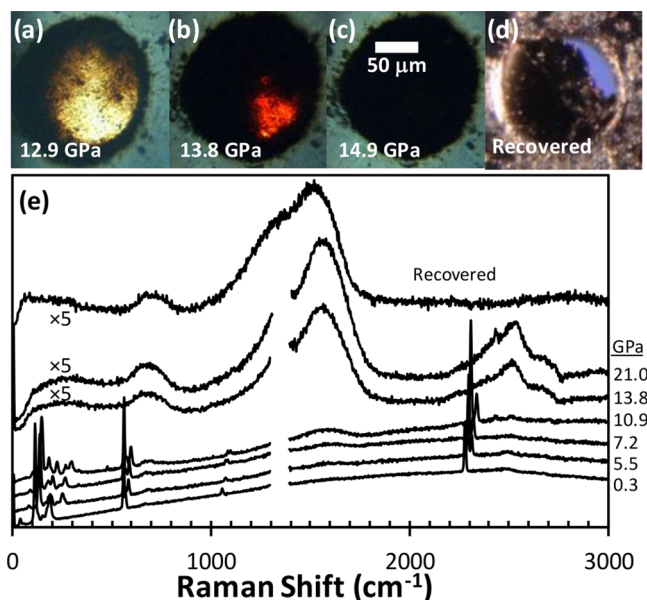
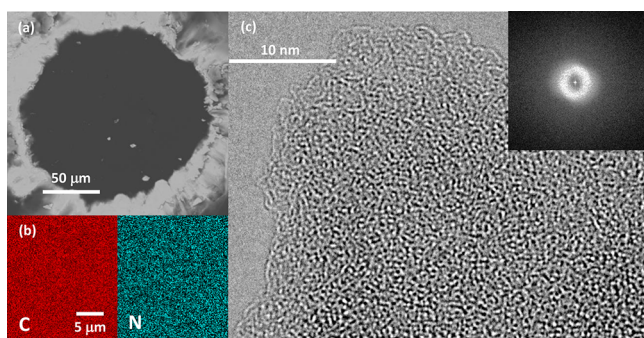


Figure 4. (a–d) *In situ* optical images of  $C(CN)_4$  collected at several pressures and recovered to 1 atm showing clear visual changes. (e) Broad-range Raman spectra of  $C(CN)_4$  with pressures up to 21 GPa and the recovered sample at 1 atm. New broad features appear above 7 GPa near  $670$  and  $1400\text{ cm}^{-1}$ . Contributions from the diamond anvils near  $1350\text{ cm}^{-1}$  were removed for clarity. Second-order scattering from the anvils is observed near  $2500\text{ cm}^{-1}$ . Raman bands from the recovered sample are centered at  $700$ ,  $1290$ , and  $1530\text{ cm}^{-1}$ .

of new  $sp^2\text{ C=N/C=C}$  bonds. The G and D peak positions at  $1323$  and  $1567\text{ cm}^{-1}$ , respectively, are consistent with other reports of amorphous carbon nitriles.<sup>43,44</sup> The presence of the D peak is an indication that ring-like structures are present.<sup>44</sup> We attribute the broad band near  $670\text{ cm}^{-1}$  to ring rotation modes, consistent with the polymerization reaction and change in bond order. The presence of ring rotation modes was previously associated with six-membered ring systems.<sup>44</sup> At ambient pressure, this ring rotation “L” mode is centered at  $700\text{ cm}^{-1}$ . Interestingly, this mode shows frequency softening behavior with increasing pressure.

After achieving a pressure  $>20$  GPa and observing the complete disappearance of nitrile Raman modes, diamond anvil cell samples were decompressed to ambient conditions for subsequent analysis of the reaction product. The microstructure and chemical composition were examined using SEM with EDS as shown in Figure 5. SEM/EDS analysis reveals that samples have a smooth, uniform texture with an average chemical composition of 59.8 at. % C, 40.0 at. % N, and 0.2 at. % O. The observed composition of  $C_5N_{3.34}$  is somewhat nitrogen deficient compared with the starting molecule ( $C_3N_4$ ), but the result indicates that no significant chemical disproportionation occurs during the transformation and that the new material is recoverable to ambient conditions and stable in air. We note that EDS analysis typically biases carbon due to column contamination (many samples are carbon coated) and other organic sources. The small amount of oxygen observed is likely due to slight surface oxidation, as all sample loadings were conducted in an inert Ar atmosphere.

HRTEM measurements conducted on the crushed sample after it was removed from the gasket show that the material is disordered on the nanometer scale and no long-range correlations are observed in the fast Fourier transform (FFT)



**Figure 5.** (A) SEM image of recovered sample in Re gasket. (B) EDS compositional maps for carbon (red) and nitrogen (blue) showing uniform chemical composition. (C) HRTEM image of recovered sample showing disorder on the atomic scale. The inset displays the FFT.

image. We note that the sample is sensitive to electron beam exposure and significant graphitization was observed after exposing the sample to the 200 kV electron beam on the time scale of minutes. This fact prevented further quantitative characterization using electron energy loss spectroscopy.

On the basis of PXRD, Raman, IR, and SEM/TEM analyses, it is clear that tetracyanomethane undergoes an irreversible polymerization process, beginning above ca. 7 GPa, and that it is indeed possible to form extended network solids through the polymerization of precursor molecules with  $sp^3$  carbon centers. The polymerization product is recoverable to ambient conditions and consists of predominantly  $sp^2$  bonds in ring-like motifs with a bulk composition similar to the starting material, as verified by Raman and EDS measurements. One plausible product of the polymerization process is the formation of distorted 1,3,5-triazine rings that would form through trimerization of three cyanide groups, each contributed by three neighboring tetracyanomethane molecules. These rings would then be linked together by the starting central  $sp^3$  carbon atom, leading to an extended network solid. It is possible for each central  $sp^3$  carbon atom to be bonded with up to four triazine rings within the idealized structure. Within the actual material, it is likely that tetracyanomethane molecules react to form multimembered rings exhibiting a variety of local environments. Because of the fact that many competitive reaction pathways are possible, the resulting material does not exhibit any long-range order. Given that the process proceeds at room temperature, it seems unlikely that any bonding changes would occur for the central  $sp^3$  starting carbon and all chemistry proceeds through the reactive nitrile groups. Larger volume scaling of the reaction product would allow for a sufficient amount of sample to be characterized by other techniques such as NMR.

## CONCLUSION

The chemical and structural changes of tetracyanomethane were examined for the first time under high-pressure conditions using Raman and IR spectroscopy and synchrotron X-ray diffraction. The results indicate that extended solid networks can be constructed from precursor molecules with built-in  $sp^3$  functionality.  $C(CN)_4$  begins to polymerize above  $\sim 7$  GPa at room temperature, and the process is completed by  $\sim 20$  GPa during compression on the time scale of hours. The polymerization product possesses a similar bulk composition to the starting material, is recoverable to ambient conditions,

and is unreactive in air. These results suggest the possibility for targeted pressure-induced polymerization with premeditated functionality designed into the precursor molecule.

## AUTHOR INFORMATION

### Corresponding Authors

\*(D.W.K.) E-mail [keefer.derek@gmail.com](mailto:keefer.derek@gmail.com); Tel 814-863-0556.

\*(T.A.S.) E-mail [tstrobel@ciw.edu](mailto:tstrobel@ciw.edu); Tel 202-478-8943.

### ORCID

Andrew Purdy: 0000-0001-5274-0818

Albert Epshteyn: 0000-0002-4489-2296

John Badding: 0000-0002-4517-830X

Timothy A. Strobel: 0000-0003-0338-4380

### Notes

The authors declare no competing financial interest.

## ACKNOWLEDGMENTS

We thank R. Hrubik for assistance with XRD measurements. This work was supported by DARPA under ARO Contract 31P4Q-13-1-0005. Portions of this work were performed at HPCAT (Sector 16), Advanced Photon Source (APS), Argonne National Laboratory. HPCAT operations are supported by DOE-NNSA under Award DE-NA0001974, with partial instrumentation funding by NSF. The Advanced Photon Source is a U.S. Department of Energy (DOE) Office of Science User Facility operated for the DOE Office of Science by Argonne National Laboratory under Contract DE-AC02-06CH11357.

## REFERENCES

- (1) Liu, A. Y.; Cohen, M. L. Prediction of New Low Compressibility Solids. *Science* **1989**, *245*, 841–842.
- (2) Teter, D. M.; Hemley, R. J. Low-Compressibility Carbon Nitrides. *Science* **1996**, *271*, 53–55.
- (3) Sandre, E.; Pickard, C. J.; Colliex, C. What Are the Possible Structures for  $CN_x$  Compounds? The Example of  $C_3N$ . *Chem. Phys. Lett.* **2000**, *325*, 53–60.
- (4) Hart, J. N.; Claeysens, F.; Allan, N. L.; May, P. W. Carbon Nitride: Ab Initio Investigation of Carbon-Rich Phases. *Phys. Rev. B: Condens. Matter Mater. Phys.* **2009**, *80*, 174111.
- (5) Wang, X.; Bao, K.; Tian, F.; Meng, X.; Chen, C.; Dong, B.; Li, D.; Liu, B.; Cui, T. Cubic Gauche-CN: A Superhard Metallic Compound Predicted Via First-Principles Calculations. *J. Chem. Phys.* **2010**, *133*, 044512.
- (6) Dong, H.; Oganov, A. R.; Zhu, Q.; Qian, G.-R. The Phase Diagram and Hardness of Carbon Nitrides. *Sci. Rep.* **2015**, *5*, 9870.
- (7) Brito, W. H.; da Silva-Araujo, J.; Chacham, H.  $G-C_3N_4$  and Others: Predicting New Nanoporous Carbon Nitride Planar Structures with Distinct Electronic Properties. *J. Phys. Chem. C* **2015**, *119*, 19743–19751.
- (8) Wang, X.; Wang, Y.; Miao, M.; Zhong, X.; Lv, J.; Cui, T.; Li, J.; Chen, L.; Pickard, C. J.; Ma, Y. Cagelike Diamondoid Nitrogen at High Pressures. *Phys. Rev. Lett.* **2012**, *109*, 175502.
- (9) Wang, X. Polymorphic Phases of  $Sp^3$ -Hybridized Superhard Cn. *J. Chem. Phys.* **2012**, *137*, 184506.
- (10) Zhu, J.; Xiao, P.; Li, H.; Carabineiro, S. A. C. Graphitic Carbon Nitride: Synthesis, Properties, and Applications in Catalysis. *ACS Appl. Mater. Interfaces* **2014**, *6*, 16449–16465.
- (11) Ong, W.-J.; Tan, L.-L.; Ng, Y. H.; Yong, S.-T.; Chai, S.-P. Graphitic Carbon Nitride ( $G-C_3N_4$ )-Based Photocatalysts for Artificial Photosynthesis and Environmental Remediation: Are We a Step Closer to Achieving Sustainability? *Chem. Rev.* **2016**, *116*, 7159–7329.
- (12) Sjöström, H.; Hultman, L.; Sundgren, J. E.; Hainsworth, S. V.; Page, T. F.; Theunissen, G. S. A. M. Structural and Mechanical

Properties of Carbon Nitride  $CN_x$  ( $0.2 < x < 0.35$ ) Films. *J. Vac. Sci. Technol., A* **1996**, *14*, 56–62.

(13) Hellgren, N.; Johansson, M. P.; Broitman, E.; Hultman, L.; Sundgren, J.-E. Role of Nitrogen in the Formation of Hard and Elastic  $Cn_x$  Thin Films by Reactive Magnetron Sputtering. *Phys. Rev. B: Condens. Matter Mater. Phys.* **1999**, *59*, 5162–5169.

(14) Holloway, B. C.; Kraft, O.; Shuh, D. K.; Kelly, M. A.; Nix, W. D.; Pianetta, P.; Hagström, S. Interpretation of X-Ray Photoelectron Spectra of Elastic Amorphous Carbon Nitride Thin Films. *Appl. Phys. Lett.* **1999**, *74*, 3290–3292.

(15) Spaeth, C.; Kühn, M.; Richter, F.; Falke, U.; Hietschold, M.; Kilper, R.; Kreissig, U. A Comparative Study of Elastic Recoil Detection Analysis (ERDA), Electron Energy Loss Spectroscopy (EELS) and X-Ray Photoelectron Spectroscopy (XPS) for Structural Analysis of Amorphous Carbon Nitride Films. *Diamond Relat. Mater.* **1998**, *7*, 1727–1733.

(16) Zheng, W. T.; Yu, W. X.; Li, H. B.; Wang, Y. M.; Cao, P. J.; Jin, Z. S.; Broitman, E.; Sundgren, J. E. Chemical Bonding, Structure, and Hardness of Carbon Nitride Thin Films. *Diamond Relat. Mater.* **2000**, *9*, 1790–1794.

(17) Sjöström, H.; Stafström, S.; Boman, M.; Sundgren, J. E. Superhard and Elastic Carbon Nitride Thin Films Having Fullerene-like Microstructure. *Phys. Rev. Lett.* **1995**, *75*, 1336–1339.

(18) Gammon, W. J.; Malyarenko, D. I.; Kraft, O.; Hoatson, G. L.; Reilly, A. C.; Holloway, B. C. Hard and Elastic Amorphous Carbon Nitride Thin Films Studied by  $^{13}C$  Nuclear Magnetic Resonance Spectroscopy. *Phys. Rev. B: Condens. Matter Mater. Phys.* **2002**, *66*, 153402.

(19) Yoo, C. S.; Nicol, M. Chemical and Phase Transformations of Cyanogen at High Pressures. *J. Phys. Chem.* **1986**, *90*, 6726–6731.

(20) Aoki, K.; Kakudate, Y.; Yoshida, M.; Usuba, S.; Fujiwara, S. Solid State Polymerization of Cyanoacetylene into Conjugated Linear Chains under Pressure. *J. Chem. Phys.* **1989**, *91*, 778–782.

(21) Tomasino, D.; Chen, J.-Y.; Kim, M.; Yoo, C.-S. Pressure-Induced Phase Transition and Polymerization of Tetracyanoethylene (TCNE). *J. Chem. Phys.* **2013**, *138*, 094506.

(22) Gou, H.; Yonke, B. L.; Epshteyn, A.; Kim, D. Y.; Smith, J. S.; Strobel, T. A. Pressure-Induced Polymerization of  $P(CN)_3$ . *J. Chem. Phys.* **2015**, *142*, 194503.

(23) Zheng, H.; et al. Polymerization of Acetonitrile Via a Hydrogen Transfer Reaction from  $CH_3$  to  $CN$  under Extreme Conditions. *Angew. Chem., Int. Ed.* **2016**, *55*, 12040–12044.

(24) Gou, H.; et al. From Linear Molecular Chains to Extended Polycyclic Networks: Polymerization of Dicyanoacetylene. *Chem. Mater.* **2017**, *29*, 6706–6718.

(25) Stavrou, E.; Lobanov, S.; Dong, H. F.; Oganov, A. R.; Prakapenka, V. B.; Konopkova, Z.; Goncharov, A. F. Synthesis of Ultra-Incompressible  $Sp^3$ -Hybridized Carbon Nitride with 1:1 Stoichiometry. *Chem. Mater.* **2016**, *28*, 6925–6933.

(26) Pickard, C. J.; Salamat, A.; Bojdys, M. J.; Needs, R. J.; McMillan, P. F. Carbon Nitride Frameworks and Dense Crystalline Polymorphs. *Phys. Rev. B: Condens. Matter Mater. Phys.* **2016**, *94*, 094104.

(27) Mayer, E. Darstellung Und Eigenschaften Von Tetracyanmethan. *Monatsh. Chem.* **1969**, *100*, 462–468.

(28) Aoki, K.; Baer, B. J.; Cynn, H. C.; Nicol, M. High-Pressure Raman Study of One-Dimensional Crystals of the Very Polar Molecule Hydrogen Cyanide. *Phys. Rev. B: Condens. Matter Mater. Phys.* **1990**, *42*, 4298–4303.

(29) Chapman, K. W.; Halder, G. J.; Chupas, P. J. Pressure-Induced Amorphization and Porosity Modification in a Metal–Organic Framework. *J. Am. Chem. Soc.* **2009**, *131*, 17546–17547.

(30) Li, K.; Zheng, H.; Ivanov, I. N.; Guthrie, M.; Xiao, Y.; Yang, W.; Tulk, C. A.; Zhao, Y.; Mao, H.-k.  $K_3Fe(CN)_6$ : Pressure-Induced Polymerization and Enhanced Conductivity. *J. Phys. Chem. C* **2013**, *117*, 24174–24180.

(31) Nesting, D. C.; Badding, J. V. High-Pressure Synthesis of  $Sp^2$ -Bonded Carbon Nitrides. *Chem. Mater.* **1996**, *8*, 1535–1539.

(32) Khazaei, M.; Arai, M.; Sasaki, T.; Kawazoe, Y. Polymerization of Tetracyanoethylene under Pressure. *J. Phys. Chem. C* **2013**, *117*, 712–720.

(33) Yamawaki, H.; Aoki, K.; Kakudate, Y.; Yoshida, M.; Usuba, S.; Fujiwara, S. Infrared Study of Phase Transition and Chemical Reaction in Tetracyanoethylene under High Pressure. *Chem. Phys. Lett.* **1992**, *198*, 183–187.

(34) Gause, E. H.; Montgomery, P. D. Hydrogen Cyanide Stability and Heat of Polymerization. *J. Chem. Eng. Data* **1960**, *5*, 351–354.

(35) Mao, H. K.; Xu, J.; Bell, P. M. Calibration of the Ruby Pressure Gauge to 800-Kbar under Quasi-Hydrostatic Conditions. *J. Geophys. Res.* **1986**, *91*, 4673–4676.

(36) Hammersley, A. Fit2d: An Introduction and Overview; ESRF Internal Report, 1998.

(37) Larson, A. C.; Von Dreele, R. B. General Structure Analysis System (GSAS); Los Alamos National Laboratory Report LAUR 86-748, 2000.

(38) Toby, B. H. Expgui, a Graphical User Interface for GSAS. *J. Appl. Crystallogr.* **2001**, *34*, 210–213.

(39) Britton, D. The Crystal Structure of Tetracyanomethane,  $C(CN)_4$ . *Acta Crystallogr., Sect. B: Struct. Crystallogr. Cryst. Chem.* **1974**, *30*, 1818–1821.

(40) Gonzalez-Platas, J.; Alvaro, M.; Nestola, F.; Angel, R. Eosfit7-GUI: A New Graphical User Interface for Equation of State Calculations, Analyses and Teaching. *J. Appl. Crystallogr.* **2016**, *49*, 1377–1382.

(41) Hester, R. E.; Lee, K. M.; Mayer, E. Tetracyanomethane as a Pseudo-(Carbon Tetrahalide). *J. Phys. Chem.* **1970**, *74*, 3373.

(42) Gardiner, D. J.; Mayer, E. Infrared-Spectra, Vibrational Assignment, Normal Coordinate Analysis and Thermodynamic Functions of Tetracyanomethane. *J. Mol. Struct.* **1973**, *16*, 173–178.

(43) Ferrari, A. C.; Rodil, S. E.; Robertson, J. Interpretation of Infrared and Raman Spectra of Amorphous Carbon Nitrides. *Phys. Rev. B: Condens. Matter Mater. Phys.* **2003**, *67*, 155306.

(44) Rodil, S. E.; Ferrari, A. C.; Robertson, J.; Milne, W. I. Raman and Infrared Modes of Hydrogenated Amorphous Carbon Nitride. *J. Appl. Phys.* **2001**, *89*, 5425.